2018

Advancement in track technology - composite foundations for increased speed and axle loads

Buddhima Indraratna
University of Wollongong, indra@uow.edu.au

Ngoc Trung Ngo
University of Wollongong, trung@uow.edu.au

Cholachat Rujikiatkamjorn
University of Wollongong, cholacha@uow.edu.au

Advancement in track technology - composite foundations for increased speed and axle loads

Abstract

The increasing demand for fast heavy haul services with greater axle loads, as well as high speed commuter trains, poses a serious challenge for the stability of tracks on the problematic ground. The use of artificial inclusions such as polymeric geosynthetics for enhanced soil-structure interaction and rubber mats made from recycled rubber tyres to absorb the strain energy and reduce ballast breakage and track damage is described in this paper as a cost-effective option. In this study, a series of large-scale laboratory tests took place to determine how well these geogrids could attenuate the impact, cyclic stress, and corresponding mitigation of ballast degradation. Comprehensive field trials took place on two full-scale rail tracks in the towns of Bulli and Singleton in New South Wales. These trials facilitated the evaluation of different types of geogrids, geocomposites and rubber mats installed in fully instrumented track sections, as well as the possible reuse of spent ballast. This paper focuses mainly on research projects at the University of Wollongong to enhance track performance by highlighting some examples of innovation from theory to practice; including case studies.

Keywords

axle, speed, increased, foundations, composite, -, technology, loads, track, advancement

Disciplines

Engineering | Science and Technology Studies

Publication Details

Indraratna, B., Ngo, N. & Rujikiatkamjorn, C. (2018). Advancement in track technology - composite foundations for increased speed and axle loads. Conference on Railway Excellence (pp. 442-451). United States: Informit.

ADVANCEMENT IN TRACK TECHNOLOGY - COMPOSITE FOUNDATIONS FOR INCREASED SPEED AND AXLE LOADS

Buddhima Indraratna[1], Ngoc Trung Ngo[1], and Cholachat Rujikiatkamjorn[1]

[1]*Centre for Geomechanics and Railway Engineering, Faculty of Engineering and Information Sciences, University of Wollongong, AUSTRALIA*

Corresponding Author: Prof Indraratna: indra@uow.edu.au

Dr. Ngoc Trung Ngo: trung@uow.edu.au

SUMMARY

The increasing demand for fast heavy haul services with greater axle loads, as well as high speed commuter trains, poses a serious challenge for the stability of tracks on the problematic ground. The use of artificial inclusions such as polymeric geosynthetics for enhanced soil-structure interaction and rubber mats made from recycled rubber tyres to absorb the strain energy and reduce ballast breakage and track damage is described in this paper as a cost-effective option. In this study, a series of large-scale laboratory tests took place to determine how well these geogrids could attenuate the impact, cyclic stress, and corresponding mitigation of ballast degradation. Comprehensive field trials took place on two full-scale rail tracks in the towns of Bulli and Singleton in New South Wales. These trials facilitated the evaluation of different types of geogrids, geo-composites and rubber mats installed in fully instrumented track sections, as well as the possible reuse of spent ballast. This paper focuses mainly on research projects at the University of Wollongong to enhance track performance by highlighting some examples of innovation from theory to practice; including case studies.

1. INTRODUCTION

Ballast is the key foundation material placed underneath sleepers to provide structural support against the high cyclic and impact stresses from fast moving trains [1-6]. Ballast is a natural or crushed granular material with a typical thickness of 250-350 mm that is placed beneath the track superstructure and above the sub-ballast (capping) or subgrade. Conventionally, coarse-sized, angular, crushed, hard stones and rocks, uniformly graded, free of dust, and not prone to cementing action is considered to be good ballast material. During operation, ballast deteriorates due to the breakage of angular corners and sharp edges, infiltration of fines from the surface, and mud pumping from the subgrade under train loading. As a result of these actions ballast becomes fouled, less angular, and its shear strength is reduced. The deterioration of ballast is one of the major contributing factors that affect the stability and longevity of railway foundations [1, 7, 8]. The adoption of various forms of synthetic inclusions such as geogrids, geocomposites and recycled rubber mats to reduce the plastic deformation and degradation of ballast has become more popular in recent years [9, 10]. These synthetic inclusions eliminate the hard interface between ballast and sleeper or the underlying formations, and allow the aggregates to bed into the relatively softer pad and thus increase the contact surface area of the ballast and reduce ballast stresses. However, studies that analyse how well these synthetic inclusions minimise ballast degradation are limited.

When ballast is fouled by breakage or infiltration of fine particles [1, 3], the interaction between them may change significantly as fine particles clog the openings (of the geogrid) to become an impermeable lubricant taht reduces the interlocking and frictional resistance between the geogrid and ballast. This paper therefore reviews recently published work using the large-scale testing apparatus and field investigations carried out at the University of Wollongong to evaluate the ability of geogrids to reduce ballast deformation and degradation.

2. EXPERIMENTAL INVESTIGATIONS

This section presents the laboratory investigations to study the shear-strain and load-deformation behaviour of coal-fouled ballast stabilised with geogrid at various degrees of fouling. A series of large-scale direct shear tests where the levels of fouling ranged from 0% to 95% Void Contamination Index (VCI), at relatively low normal stresses varying from 15kPa to 75kPa were conducted and details are presented in the following sections.

2.1 Ballast Fouling

During track operations, fine particles can accumulate within the ballast voids due to: (i) the breakage of sharp angular projections (corners), (ii) fines infiltrating from the surface,

and (iii) pumping of soft saturated subgrade under excessive cyclic loads [11]. As the fouling material occupies the free voids of ballast it slowly impedes the drainage capacity of the track. Most ballast fouling (around 76%) originates from the fracture and abrasion of ballast particles, followed by 13% due to infiltration from the subballast, 7% infiltration from the surface, 3% from subgrade intrusion, and 1% from sleeper wear [3, 12]. In Australia, the intrusion of coal fines and ballast breakage are the major sources of ballast fouling because they contribute about 70-95% and 5-30%, respectively [13]. In low-lying coastal areas where the subgrade is usually saturated, the finer silt and clay particles are pumped up into the ballast layer as 'slurry' under train loading, however this problem can be eliminated if a properly graded filtration layer or geosynthetics are placed underneath the ballast layer [4, 14].

2.2 Assessment of Ballast Fouling

There are several fouling indices available for quantifying ballast fouling. Selig and Water [3] introduced a fouling index (FI) which is a summation of the percentage (by weight) of fouled ballast passing through a 4.75 mm (No. 4) sieve and 0.075 mm (No. 200) sieve. Feldman and Nissen [15] proposed a Percentage Void Contamination (PVC) to overcome some of the limitations associated with FI; PVC is defined as the ratio of the bulk volume of fouling material to the volume of voids in clean ballast. Since the mass based index could give a false quantification of fouling when the fouling material (e.g. coal) has a low specific gravity, this fouling index has become more popular in QLD, Australia because the common source of fouling is coal spillage from the wagons transporting coal from the coal mines. Since this method does not represent the real volume of fouling that may exist in the field, Tennakoon et al. [11] modified this fouling index by incorporating the real volume of fouling and then introducing a new fouling index called the Void Contaminant Index (*VCI*):

$$VCI = \frac{(1+e_f)}{e_b} \times \frac{G_{sb}}{G_{sf}} \times \frac{M_f}{M_b} \times 100 \qquad (1)$$

where, e_b is the void ratio of clean ballast, e_f is the void ratio of fouling material, G_{sb} is the specific gravity of the ballast material, G_{sf} is the specific gravity of the fouling material, M_b is the dry mass of clean ballast, and M_f is the dry mass of the fouling material. There is a significant variation in the void ratio (e_f), specific gravity (G_{sf}), and gradation characteristics of fouling materials, but the *VCI* can include all of these variations; therefore *VCI* is used here to quantify the amount of fouling.

2.3 Large-scale Direct Shear Testing

The large scale direct shear apparatus is a 300mm x 300 mm by 200 mm high steel box (Figure 1). The ballast collected from Bombo quarry, New South Wales, Australia has been cleaned and sieved according to Australia Standards AS 2758.7 [16]. Coal fines are used as fouling contaminant and the Void Contamination Index (*VCI*) is used to measure the degree of fouling. Large-scale direct shear tests for fresh and fouled ballast reinforced by the 40 mm x 40 mm geogrid

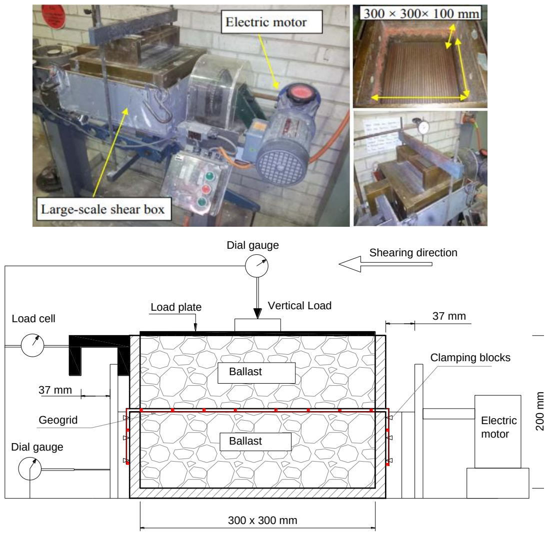

Figure 1: Large-scale direct shear box

have been carried out to a displacement of Δh=37mm; the results are discussed elsewhere by Indraratna *et al.* [9]. These test results show that the peak shear stress of ballast increases with an increase in normal stress and then it decreases with an increasing level of fouling (i.e. increased *VCI*). Strain softening and dilation has also been obtained for all the tests, where a higher normal stress σ_n, a greater shear strength, and smaller dilations are observed. Figure 2 shows that the coal fines reduce the peak shear stress of reinforced and unreinforced ballast assemblies by coating the surfaces of ballast grains and thus inhibiting inter-particle friction and reducing shearing resistance at the geogrid-ballast interface. Tutumluer *et al.* [7] noted that the railway ballast they measured in the laboratory has similar shear stress-strain responses. The variations of normalised peak shear stress (τ_p/σ_n) and the apparent angle of shearing resistance (ϕ) with *VCI* of fouled ballast assemblies with and without geogrid reinforcement are shown in Figure 2. Note that the coal fines steadily reduce the peak shear

stress of a fouled ballast assembly, which then reduces the apparent angle of shearing resistance. This reduction of (τ_p/σ_n) due to the coal fines is significant when the *VCI* is less than 70%, but it becomes marginal when the *VCI* is higher. The apparent friction angles measured in this study vary from 46^0 to 65^0 depending on the normal stress applied.

2.4 Geosynthetics-ballast interface

The influence that the geometry and opening aperture size of geosynthetics and confining pressure has on the interface of a geosynthetics-reinforced ballast composite

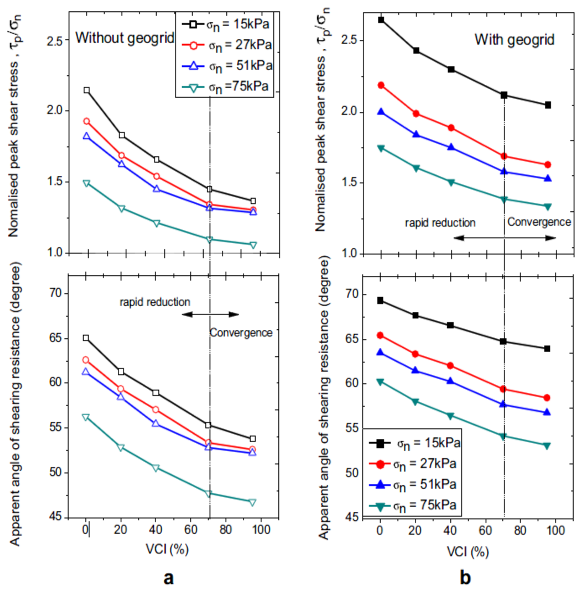

Figure 2: Effect of *VCI* on shear strength and angle of shearing: (a) without geogrid, and (b) with geogrid

(*after Indraratna et al. [9]*)

the assembly has been carried out by Indraratna et al. [17]. In this study, seven types of geosynthetics, namely G1 to G7 (Table 1) with square, rectangular, and triangular geometry and different size apertures (i.e. 36 mm to 70 mm) are tested using the large-scale direct shear test under normal stresses of 26.3 kPa to 61 kPa. All these tests are at a shear displacement of 36 mm because it corresponds to a horizontal strain of 12%. The effect of an applied normal stress on the internal friction angle of ballast reinforced by different types of geosynthetics is shown in Figure 3a where the friction angle of ballast decreases from 64^0 to 59^0 when the normal stresses increase from 26 to 61kPa. It is well known that the friction angle of granular materials decreases as the confining pressure increases, and similarly, the internal friction angle of ballast-geogrid interfaces also decreases as the normal stresses increase; this trend is similar to the unreinforced ballast.

The actual improvement in the behaviour of ballast-geogrid interfaces can be determined in terms of the interface efficiency factor which is defined as the ratio of the shear strength of the interface to the internal shear strength of the ballast:

$$\sigma = \frac{\tan\delta}{\tan\varphi} \qquad (2)$$

where, δ is the apparent friction angle of the interface and φ is the friction angle of the ballast. Note that the cohesion intercept for ballast materials is omitted.

Geogrid type	Aperture shape	Aperture size (mm)	Tensile strength (kN/m)
G1	Square	38 × 38	30
G2	Triangle	36	19
G3	Square	65 × 65	30
G4	Rectangle	44 × 42	30
G5	Rectangle	36 × 24	30
G6	Square	33 × 33	40
G7	Rectangle	70 × 110	20

Table 1: Physical characteristics of the geogrids used in this study.

The influence that the size of the geogrid aperture has on the shear strength of the ballast-geogrid interface is shown in Figure 3b. Here the value of α is a function of the A/D_{50} ratio, where α increases with A/D_{50} until it attains a maximum value of 1.16 at A/D_{50} of 1.21, and then it decreases towards unity as A/D_{50} approaches 2.5. The value of α <1 indicates an ineffective interlocking of particles, whereas α >1 indicates acceptable interlocking, which helps to increase the shear strength. In other words, the A/D_{50} value where α =1 is the minimum condition needed to generate the benefits of geogrid reinforcement. Based on the variation of α, an optimum interlock zone is defined where the interface efficiency factor is between 0.95 to 1.2. The value of α attains a maximum of 1.16 at an optimum A/D_{50} ratio of about 1.20. This study indicates that the minimum and maximum size apertures of geogrid to optimise the shear strength are $0.95D_{50}$ and $2.50D_{50}$, respectively, and the optimum size aperture of geogrid is approximately 1.2-1.3 D_{50}.

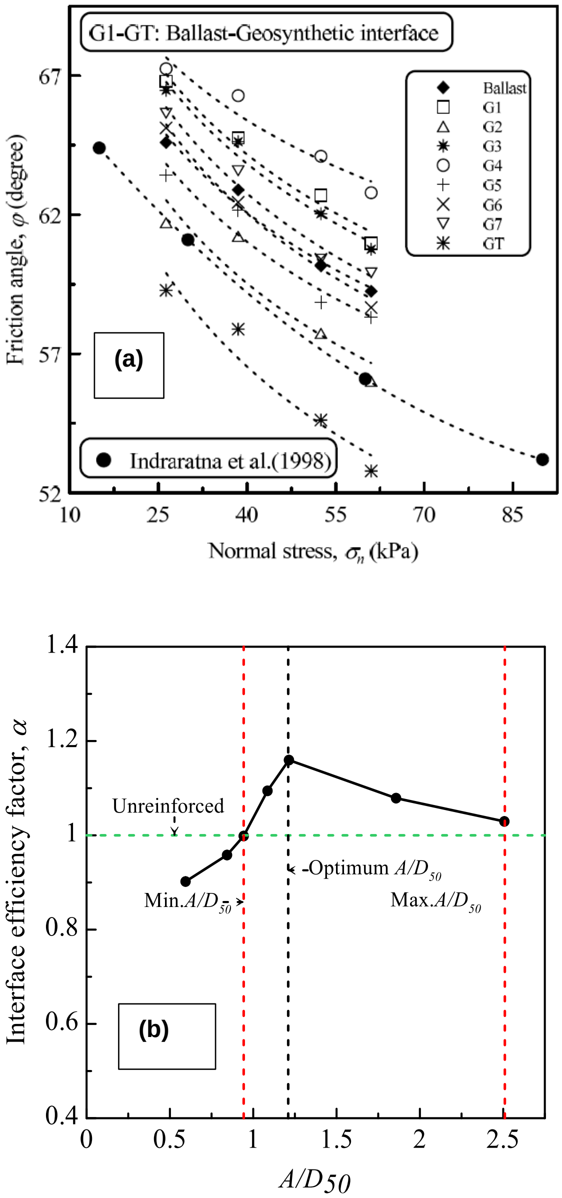

Figure 3: (a) Variation of friction angle of ballast-geosynthetic interfaces with normal stress; (b) Interface efficiency factor (α) versus A/D_{50}

2.5 Ballast behaviour – Monotonic and Cyclic Loading Research Findings

Several researches have been presented on the effects that the loading characteristic (i.e. monotonic or cyclic loads) has on the stress and strain of railway ballast ([5, 18, 19]. Following extensive laboratory tests, the volumetric strains measured at different confining pressures are shown in Figure 4 where dilation (volume increase) occurs in the ballast samples for most confining pressures under monotonic loads. Although similar ballast materials were tested in the same large-scale triaxial apparatus, they all exhibited different volumetric strain responses under different loading conditions. However, those ballast assemblies which underwent cyclic loads (i.e. confining pressure higher than 30 kPa) experienced pronounced compression, possibly due to the reorientation and rearrangement of particles which occurs during cyclic loading which generates a denser (compressing) or looser (dilating) packing assembly [10, 20]. Those specimens subjected to low confinement exhibit purely dilative behaviour, whereas the reverse occurs for assemblies with higher confining pressures under monotonic loads.

2.6 Large-scale Cyclic Testing for Geogrid-Reinforced Ballast

This section presents the results of an experimental study of coal-fouled ballast reinforced with geogrid, at various degrees of coal fouling and subjected to cyclic loading. A novel large-scale Process Simulation Testing Apparatus (PSTA) is used to realistically simulate fouled rail track conditions (Figure 5). Details of the PSTA by Indraratna et al., can be found elsewhere [4]. A 150 mm thick layer of dry gravel and sand acts as subballast and is compacted to achieve a representative field unit weight of approximately 19.5 kN/m^3. A layer of geogrid (40 mm × 40 mm) is then placed onto the subballast layer, which is then covered by ballast and compacted to a field unit weight of 15.5 kN/m3. Ballast aggregates are placed in multiple layers to a total thickness of 300 mm, each of which was compacted with a handheld vibratory compactor to reach the desired unit weight. To simulate fouled ballast, there is a predetermined weight of coals over each layer that will meet the designated *VCI*. These coal fines then migrate and accumulate into voids between the particles of ballast under gravity and compaction. A total of 10 tests were carried out for coal-fouled ballast with and without the inclusion of geogrid, and with a *VCI* between 0% and 70%. All the tests had a frequency of 15 Hz, a maximum applied cyclic stress of 420 kPa, and experienced up to 500,000 load cycles. Every instrument was calibrated before being connected to an electronic DT800 data logger controlled by a host computer that accurately recorded the settlement, distributions of stress, and lateral

displacement of the associated walls at pre-determined time intervals.

Figure 6 presents the final lateral displacement and vertical settlement of coal-fouled ballast

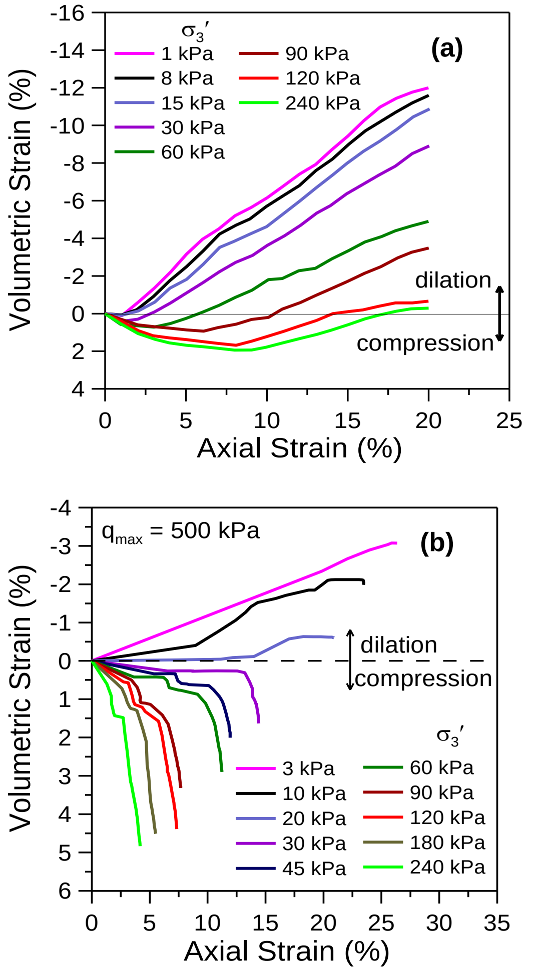

Figure 4: Volumetric strain of ballast tested under: (a) monotomic load; (b) cyclic load *(after Indraratna et al. [1]; Lackenby et al. [6]*

measured in the laboratory with and without geogrid reinforcement. Here the geogrid reduces the lateral displacement of fresh and fouled ballast quite considerably because the ballast creates a strong mechanical interlock with the geogrid; this interlocking may enable the geogrid to act as a fixed boundary that reduces deformation. This observation agrees with the previous study by McDowell et al. [21] where the discrete element method (DEM) revealed that the geogrid acts like an interlock by forming a stiffened zone inside the ballast assembly. An increase in the *VCI* markedly increases the horizontal displacement and larger settlement. Indeed, as fouling increases, the coal fines act as a lubricant which assists the particles to slide and/or roll and thus increases formation. Figure 6d shows how the geogrid reduces the deformation of ballast, as elucidated by the values of R. Note that the effect of geogrid becomes marginal if the *VCI* exceeds 40%, essentially, geogrid performs best when placed in a fresh ballast assembly (approximately 52% and 32% reduction for lateral and vertical deformation, respectively), but it's performance decreases significantly with an increase of *VCI* (approximately 5% and 12% reduction for lateral and vertical deformation for *VCI*=40%).

3. USE OF GEOSYNTHETICS FOR RAIL INFRASTRUCTURE

3.1 Application of Geosynthetics at Bulli Track

An experimental section of track was built in Bulli, along RailCorp's South Coast Track, NSW to study track performance via train-induced stresses, track deformation, and the effects of geosynthetics [22-24]. This section of instrumented track is subdivided into four sections, 15 m long (Figure 7). The ballast and sub-ballast layers are 0.3 and 0.15 m thick, respectively; sections 1 and 4 have fresh and recycled ballast without geosynthetic reinforcement [4], and there is a geocomposite at the ballast-sub-ballast interface in Sections 3 and 4. The particle size distribution of fresh ballast follows Technical Specification TS 3402 (RailCorp, Sydney). Recycled ballast came from spoil tips of a recycled plant in Chullor ', Sydney. The sub-ballast materia (b) ıtegorised as a sand-gravel mixture, and the geocomposite layers are a combination of biaxial geogrids and nonwoven geotextile layers. The technical specifications of various materials used during construction are reported in Indraratna et al. [4]. The experimental sections are monitored as follows: the vertical and horizontal deformation is obtained by settlement plates (Figure 7d) and digital displacement transducers installed at the sleeper-ballast and ballast-sub-ballast interfaces, respectively [2].

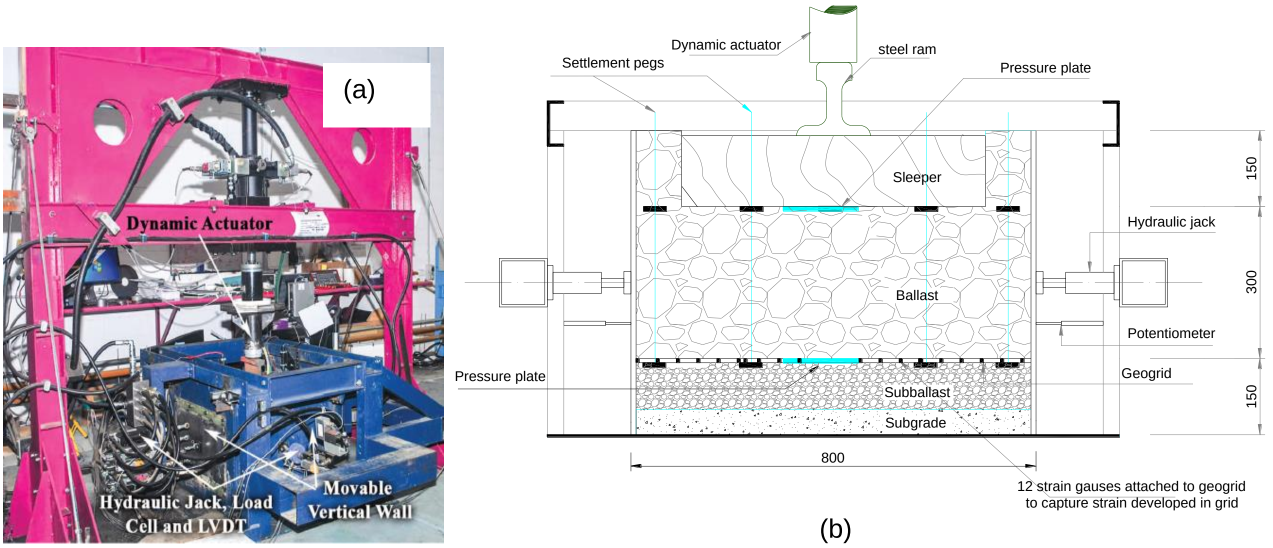

Figure 4: (a) Large-scale Process Simulation Testing Apparatus (PSTA); (b) Schematic cross section of the ***PSTA (after Indraratna et al. [1])***

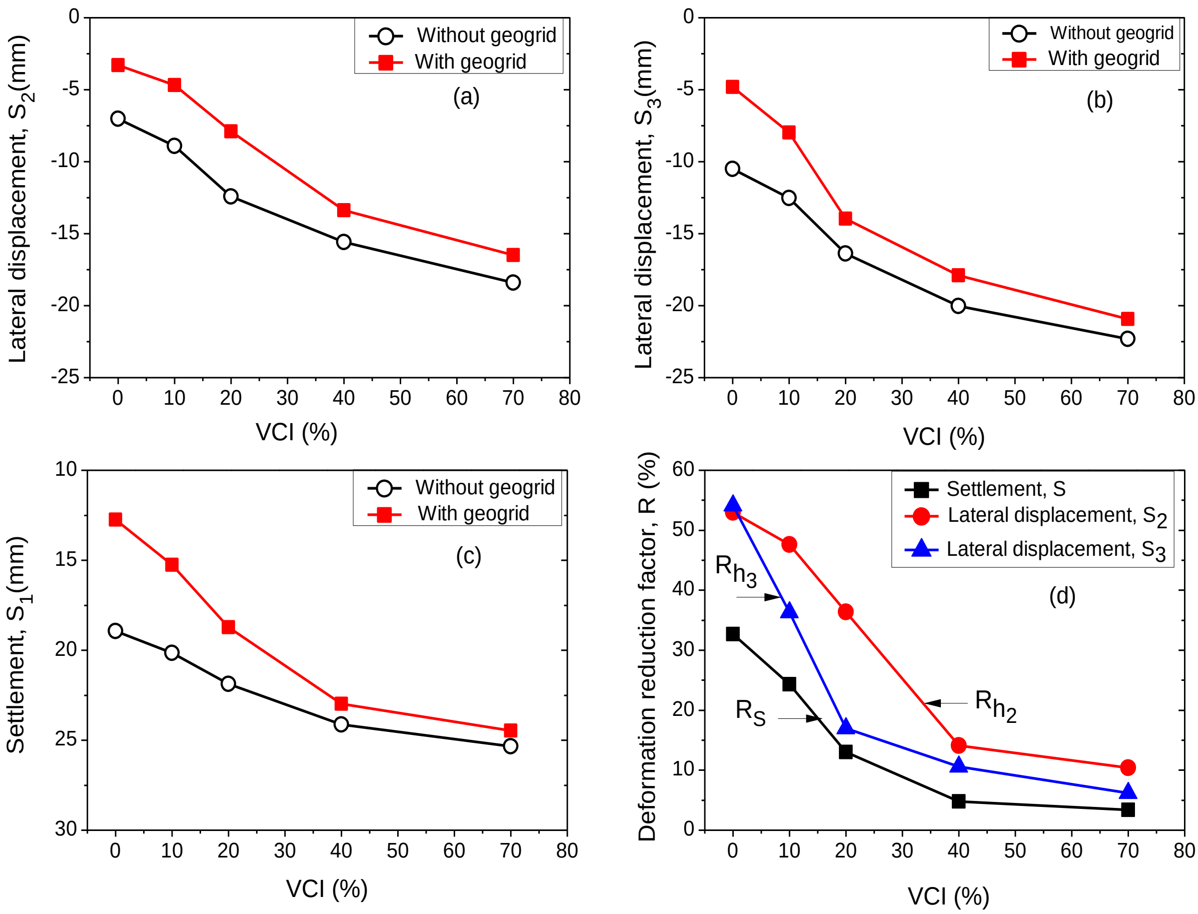

Figure 5: Deformation of fresh and fouled ballast with and without geogrid: (a) lateral displacement S2; (b) lateral displacement S3; (c) settlement S; (d) deformation reduction factor, R (modified after Indraratna et al. 2013 ***(after Indraratna et al. [1])***

3.2 Traffic induced stresses in ballast

Figure 8a shows the peak cyclic vertical (σ_v) and lateral (σ_l) stresses recorded at Section 1 (i.e. fresh ballast without geocomposite) after the passage of a coal train with an axle load of 25 tonnes. Here the peak cyclic vertical stress (σ_v) decreased by 73 % and 82 % at depths of 300 mm and 450 mm, respectively. Moreover, σ_l only decreased marginally with depth, which implies that artificial inclusions are needed for additional restraints. While most of the peak cyclic vertical stresses (σ_v) are almost 230 kPa, one value of σ_v reached 415 kPa, as shown in Figure 8b; this was later found to be associated with a wheel flat, thus proving that much larger stresses are exerted by wheel imperfections that could generate large impact forces. The resulting particle breakage could be mitigated by a shock mat, as presented by Indraratna et al. [10] in the Singleton study.

where N_t, A_t and N_c are the numbers of load cycles per MGT, the axle load in tonnes, and the number of axles per load cycle. When this relationship is used for a traffic tonnage of 60 MGT per year and four axles per load cycle, an axle load of 25 tonnes gives 600,000 load cycles per MGT. A simple survey technique is then used to record changes in the reduced level of the tip of the settlement pegs. The average ballast settlements against the number of load cycles (N) are shown in Figure 9. Unlike fresh ballast, recycled ballast has less vertical and lateral deformation, possibly due to its moderately graded particle size distribution - PSD (C_u = 1.8) compared to the very uniform PSD (C_u = 1.5) of fresh ballast. These results also indicate that geocomposite reinforcement reduces the vertical (S_v) and lateral (S_l) deformation of fresh ballast by around 33 % and 49 %, respectively, as well as reducing the vertical (S_v) and lateral (S_l) deformation of recycled ballast by about 9 %

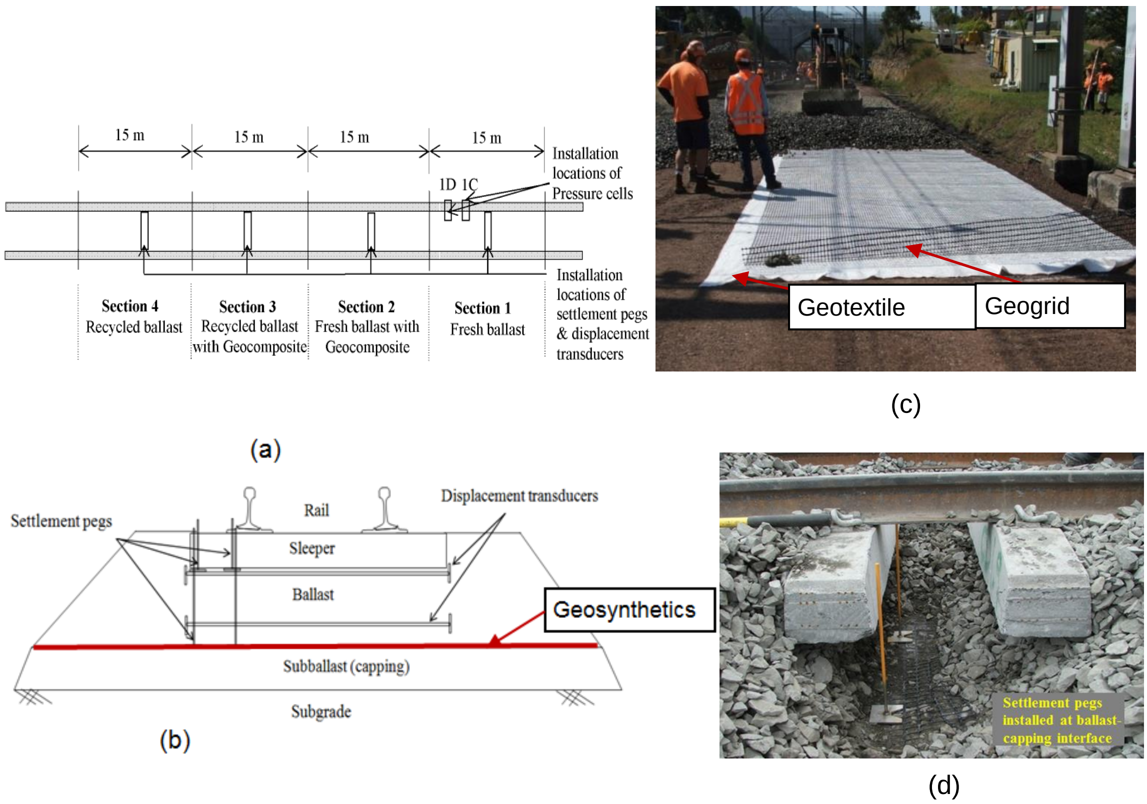

Figure 6: (a) Construction of track sections; (b) Installing vertical settlement pegs and displacement transducers; (c) installation of geosynthetics; (d) Instrumentations

3.3 Ballast deformation

In the field, vertical and horizontal deformation is measured against time, so a relationship between the annual rail traffic in million gross tons (MGT) and axle load (A_t) is needed to determine the number of load cycles N, as proposed by Selig and Waters (1994). This relationship is expressed as: $N_t = 106/(A_t \times N_c)$,

and 11 %, respectively. Lateral deformation is one of the most important indices, and the geocomposite reinforcement markedly improved the lateral stability because the geogrid enhances mechanical interlocking with the ballast. This result enables the ballast layer to distribute the load and substantially reduce settlement under high repeated loading.

4. CONCLUSION

This paper presented a geotechnical perspective of railroad performance with special reference to the deformation and degradation of track substructure through investigations. It describes the key research findings of the stress-strain responses of ballast subject to static and cyclic loading, as well as the degradation of ballast and its implications on the design and performance of tracks. The influence of confining pressure, and train speed (frequency) on the degradation and deformation of railroad ballast under cyclic loading was investigated by large-scale ballast testing apparatus. These large scale triaxial tests indicate that geogrid increases the shear strength and apparent angle of shearing resistance, but only slightly decreases the vertical displacement of a composite geogrid-ballast

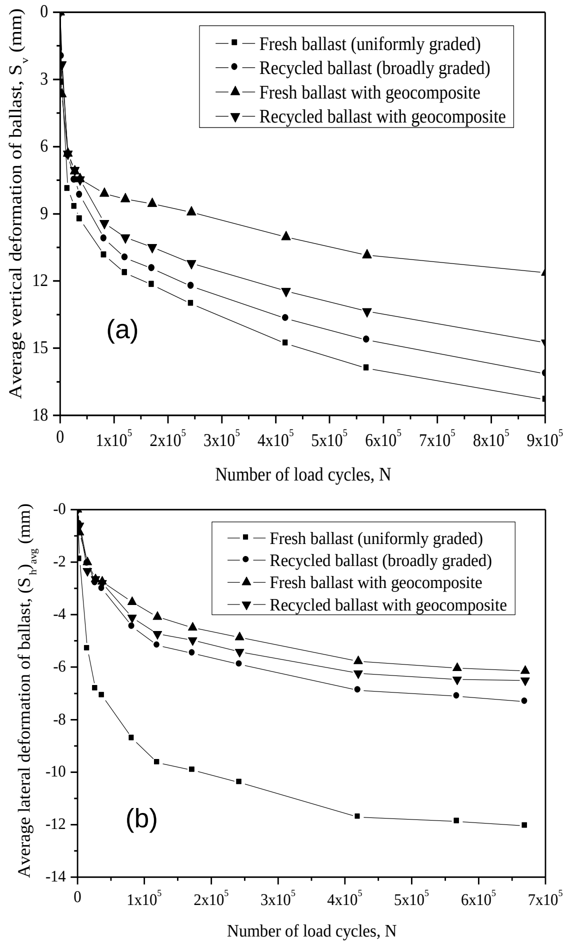

Figure 7: Average deformations of the ballast layer: (a) vertical; (b) lateral *(data sourced from Indraratna et al. [2])*.

system. However, when the ballast is fouled by coal fines, the benefits of geogrid reinforcement decrease in proportion to the increasing level of fouling. It is also noted that the normalised aperture ratio, (A/D_{50}) had a profound influence on the interface efficiency factor (α). The best size geogrid aperture to optimise the interface shear strength is around 1.20D_{50}. The maximum and minimum sized apertures needed to attain the beneficial effects of geogrids are 0.95D_{50} and 2.50D_{50}, respectively. DEM simulations for large-scale direct shear tests were carried out on fresh and fouled ballast (*VCI*=40%) to examine how geogrids improve its performance.

The field performance of ballasted rail tracks with geosynthetic reinforcement is discussed in this paper. The performance of instrumented ballasted tracks at Bulli was evaluated with different types of ballast and geosynthetic reinforcement. The results of the Bulli field study indicated that the use of geocomposites as reinforcing elements for tracks with recycled ballast proved to be a feasible and affective alternative.

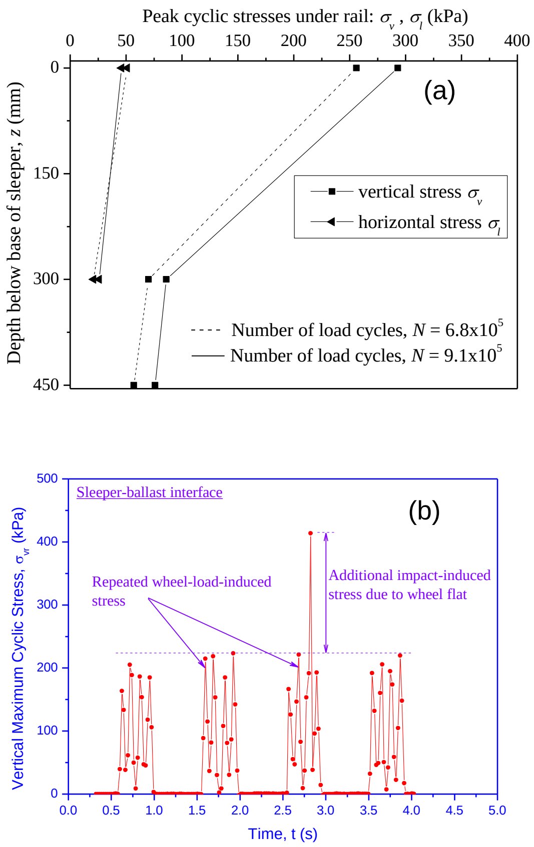

Figure 8: Cyclic stresses induced by coal train with wagons (100 tonnes): (a) variation of stresses with depth, (b) additional stress due to wheel flat *(data sourced from Indraratna et al. [2])*.

5. ACKNOWLEDGEMENTS

The research projects on ballasted rail tracks and geosynthetics are supported by the Australian Research Council (ARC), while the collaborations with industry partners facilitated

the application of putting theory into practice. In this respect, the authors greatly appreciate the financial support from the Rail Manufacturing Cooperative Research Centre (funded jointly by participating rail organisations and the Australian Federal Government's Business Cooperative Research Centres Program) through Project R2.5.1 - Performance of recycled rubber inclusions for improved stability of railways. The Authors would like to thank the Australasian Centre for Rail Innovation (ACRI) Limited, and Tyre Stewardship Australia Limited for providing the financial support needed to undertake this research. The Authors sincerely acknowledge Sydney Trains, Australian Rail Track Corporation (ARTC), among others. The timely and ongoing assistance of David Christie (formerly Senior Geotechnical Consultant, RailCorp), Tim Neville (ARTC) and Michael Martin (Aurizon/QLD Rail) is gratefully acknowledged. Salient contents from past articles (ASCE Journal of Geotechnical & Geoenvironmental Engineering, Computers and Geotechnics, Int. J. of Geomechanics, Geotechnique) have been reproduced here with kind permission from the original sources.

6. REFERENCES

1. Indraratna, B., N.T. Ngo, and C. Rujikiatkamjorn, Deformation of coal fouled ballast stabilized with geogrid under cyclic load. Journal of Geotechnical and Geoenvironmental Engineering, 2013. 139(8): p. 1275-1289.

2. Indraratna, B., S. Nimbalkar, D. Christie, C. Rujikiatkamjorn, and J.S. Vinod, Field assessment of the performance of a ballasted rail track with and without geosynthetics. Journal of Geotechnical and Geoenvironmental Engineering, ASCE, 2010b. 136(7): p. 907–917.

3. Selig, E.T. and J.M. Waters, Track geotechnology and substructure management. 1994: Thomas Telford, London.

4. Indraratna, B., W. Salim, and C. Rujikiatkamjorn, Advanced Rail Geotechnology - Ballasted Track. 2011a: CRC Press, Taylor & Francis Group, London, UK

5. Indraratna, B., D. Ionescu, and D. Christie, Shear Behaviour of Railway Ballast based on Large Scale Triaxial Testing. Journal of Geotechnical and Geoenvironmental Engineering, 1998. 124(5): p. 439-449.

6. Lackenby, J., B. Indraratna, G.R. McDowell, and D. Christie, Effect of confining pressure on ballast degradation and deformation under cyclic triaxial loading. Geotechnique, 2007. 57(6): p. 527–536.

7. Tutumluer, E., W. Dombrow, and H. Huang. Laboratory characterization of coal dust fouled ballast behaviour. in AREMA 2008 Annual Conference & Exposition. 2008. Salt Lake City, UT, USA.

8. Suiker, A., E. Selig, and R. Frenkel, Static and cyclic triaxial testing of ballast and subballast. J. Geotech. Geoenviron. Eng., 2005: p. 771.

9. Indraratna, B., N.T. Ngo, and C. Rujikiatkamjorn, Behavior of geogrid-reinforced ballast under various levels of fouling. Geotextiles and Geomembranes, 2011b. 29(3): p. 313-322.

10. Indraratna, B., S.S. Nimbalkar, N.T. Ngo, and T. Neville, Performance improvement of rail track substructure using artificial inclusions – Experimental and numerical studies. Transportation Geotechnics, 2016. 8: p. 69-85.

11. Tennakoon,Indraratna, Rujikiatkamjorn,Nimbalkar, Neville, The Role of Ballast-Fouling Characteristics on the Drainage Capacity of Rail Substructure. Geotechnical Testing Journal, 2012. 35(4): 1-11.

12. Dombrow, W., H. Huang, and E. Tutumluer. Comparison of coal dust fouled railroad ballast behavior- granite vs. limestone. in Bearing Capacity of Roads, Railways and Airfields, Proceedings of the 8th International Conference (BCR2A'09). 2009. Taylor & Francis Group.

13. Feldman, F. and D. Nissen. Alternative testing method for the measurement of ballast fouling: Percentage Void Contamination. in Conference on Railway Engineering, RTSA. 2002. Wollongong, Australia.

14. Trani, L.D.O. and B. Indraratna, Assessment of subballast filtration under cyclic loading. Journal of Geotechnical and Geoenvironmental Engineering, 2010. 136(11): p. 1519-1528.

15. Feldman, F. and D. Nissen. Alternative testing method for the measurement of ballast fouling. in Conference on Railway Engineering. 2002. Wollongong: RTSA.

16. AS 2758.7 (1996) Aggregates and rock for engineering purposes, Part 7. Railway Ballast. Standard Australia, 1996. NSW, Australia.

17. Indraratna, B., S.K.K. Hussaini, and J.S. Vinod, On the shear behaviour of of ballast-geosynthetic interfaces. Geotechnical Testing Journal, 2012. 35(2): p. 1-8.

18. Ngo, N.T., B. Indraratna, C. Rujikiatkamjorn, and M.M. Biabani, Experimental and Discrete Element Modeling of Geocell-Stabilized Subballast Subjected to Cyclic Loading. Journal of Geotechnical and Geoenvironmental Engineering, 2016. 142(4): p. 04015100.

19. Indraratna, B., N.T. Ngo, C. Rujikiatkamjorn, and J. Vinod, Behaviour of fresh and fouled railway ballast subjected to direct shear testing - a discrete element simulation. International Journal of Geomechanics, ASCE, 2014. 14(1): p. 34-44.

20. Ngo, N.T., B. Indraratna, and C. Rujikiatkamjorn, Micromechanics-Based Investigation of Fouled Ballast Using Large-Scale Triaxial Tests and Discrete Element Modeling. Journal of Geotechnical and Geoenvironmental Engineering. 134(2): p. 04016089.

21. McDowell, G.R., O. Harireche, H. Konietzky, S.F. Brown, and N.H. Thom, Discrete element modelling of geogrid-reinforced aggregates. Proceedings of the ICE - Geotechnical Engineering 2006. 159(1): p. 35-48.

22. Indraratna, B., Ngo, N. T., Nimbalkar, S., and Rujikiatkamjorn, C., “Two Decades of Advancement in Process Simulation Testing of Ballast Strength, Deformation, and Degradation,” Railroad Ballast Testing and Properties, ASTM STP1605, T. D. Stark, R. Szecsy, and R. H. Swan, Jr., Eds., ASTM International, West Conshohocken, PA, 2018, pp. 1–28,

http://dx.doi.org/10.1520/STP160520170029

23. Rujikiatkamjorn, C., Indraratna, B., Ngo, N.T. and Coop, M. (2012). "A laboratory study of railway ballast behaviour under various fouling degree." The 5th Asian Regional Conference on Geosynthetics, pp: (pp. 507-514).

24. Indraratna, B., Sun, Q., Ngo, N.T. and Rujikiatkamjorn, C. (2017). "Current research into ballasted rail tracks: model tests and their practical implications." Australian Journal of Structural Engineering, 18(3), pp: 204-220.